Signal Processing 91 (2011) 2213–2221

Contents lists available at ScienceDirect

Signal Processing

journal homepage: www.elsevier.com/locate/sigpro

A tracker-aware detector threshold optimization formulation for tracking maneuvering targets in clutter

Murat Şamil Aslan [a,*], Afşar Saranlı [b]

[a] TÜBİTAK BİLGEM UEKAE İLTAREN, Şehit Mu. Kur. Yzb. İlhan Tan Kışlası, 2432. cad., 2489. sok., Ümitköy, Ankara 06800, Turkey
[b] Department of Electrical and Electronics Engineering, Middle East Technical University, Ankara 06531, Turkey

ARTICLE INFO

Article history:
Received 26 October 2010
Received in revised form
30 March 2011
Accepted 1 April 2011
Available online 12 April 2011

Keywords:
Radar
Tracker-aware
Detection
Threshold optimization
Interacting multiple model (IMM)
Probabilistic data association (PDA)
Modified-Riccati equation (MRE)
Hybrid conditional averaging (HYCA)

ABSTRACT

In this paper, we consider a tracker-aware radar detector threshold optimization formulation for tracking maneuvering targets in clutter. The formulation results in an online method with improved transient performance. In our earlier works, the problem was considered in the context of the probabilistic data association filter (PDAF) for non-maneuvering targets. In the present study, we extend the ideas in the PDAF formulation to the multiple model (MM) filtering structures which use PDAFs as modules. Although our results are general for the MM filters, our simulation experiments apply the proposed solution in particular for the interacting multiple model PDAF (IMM-PDAF) case. It is demonstrated that the suggested formulation and the resulting optimization method exhibits notable improvement in transient performance in the form of track loss immunity. We believe the method is promising as a detector-tracker jointly-optimal filter for the IMM-PDAF structure for tracking maneuvering targets in clutter.

1. Introduction

The radar signal and data processing is usually viewed as a concatenation of two subsystems: *Signal processing* followed by *tracking* (also called *information processing* [1] or *data processing* [2,3]) as illustrated in Fig. 1. The common approach to the signal processing side is first to specify a desired (or acceptable) false alarm probability (P_{FA}^d) for the detector and then maximize the probability of detection (P_D) with this constraint [4]. The value of P_{FA}^d is usually selected in view of the radar processor's computational capacity in handling maximum number of false alarms. Although this seems a reasonable criterion, it is only a heuristic one. It neither accounts for the properties of the downstream tracker, nor it cares for an overall performance objective. *Tracker-aware detector threshold optimization* (TA-DETOP) aims at optimally selecting this *operating false alarm probability* (which in turn determines the detector operating point and the detection threshold), so that the output performance of the downstream tracker, hence of the combined target state estimation system, is maximized. This structure constitutes a form of feedback from the downstream tracker to the upstream detector as illustrated in Fig. 1.

The line of study devoted to the optimization of the radar detector by using such a feedback from the information processing subsystem to the signal processing subsystem has been pioneered by Fortmann et al. [5]. The primary motivation in [5] is to find a *deterministic* recursion for the covariance of the probabilistic data association filter (PDAF) [6], in a way similar to the one for the Kalman filter, which is the standard Riccati equation (SRE). It turns out that the end product, the *modified Riccati equation* (MRE), differs from the SRE only by a scalar variable [5], called the *information reduction*

* Corresponding author.
E-mail addresses: murat.aslan@iltaren.tubitak.gov.tr, msaslan@gmail.com (M. Şamil Aslan), afsars@metu.edu.tr (A. Saranlı).

0165-1684/$ - see front matter © 2011 Elsevier B.V. All rights reserved.
doi:10.1016/j.sigpro.2011.04.004

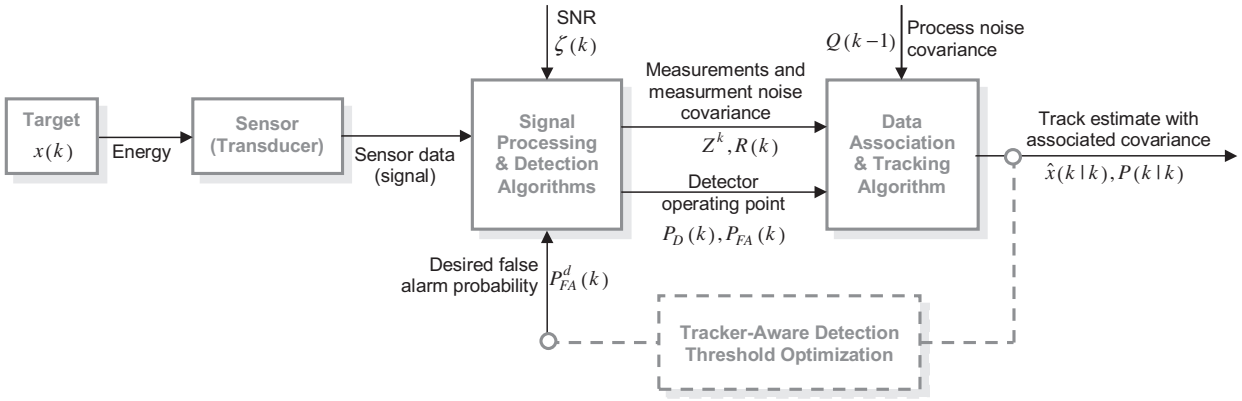

Fig. 1. Block diagram of conventional radar signal and data processing with a decoupled feed-forward structure. Tracker-aware detection threshold optimization introduces a feedback from tracker to the detector as illustrated in the figure.

factor (IRF) [1]. This scalar depends explicitly on the detector operating point, i.e., the probability of false alarm (P_{FA}) and the probability of detection (P_D). Using this dependence, the authors of [5] introduced a graphical technique for the optimization of the detector thresholds for systems which are linear and *time-invariant*. Time-invariance assumption makes this technique *static* in the sense that the optimization is based on the steady-state solution of the MRE. The method proposed is based on iterating the MRE to its steady-state, for a possible range of signal-to-noise ratio (SNR) values. The optimum detector operating points can be found and tabulated offline, and then used when necessary in an online application with varying SNR conditions.

When the steady-state analysis is inappropriate, such as time-varying or nonlinear systems, a suggested solution is to apply the same methodology by iterating the MRE not to its steady-state but for n steps into the future [5]. In the case of $n=1$, this leads to a *dynamic* (also called *adaptive* [7]) *threshold optimization* (DTOP) scheme. In [7], Gelfand et al. proposed two such problems, namely, *prior* and *posterior* threshold optimization, where they minimize the mean-square state estimation error over detection thresholds, based on the measurements up to the previous (prior) and current (posterior) time steps, respectively. It was further shown that for the *prior* case, the problem reduces into a single line search which maximizes the IRF [7]. Due to the claimed mathematical intractability of obtaining a full closed-form solution, in [7], this problem was solved using iterative numerical optimization techniques, such as Golden-Section and Fibonacci Search methods [8]. In [9], the same problem is solved in an approximate closed-form for a special case of Neyman–Pearson (NP) detector using a functional approximation introduced by [10]. It was shown that this approximate closed-form solution leads to considerable reduction in computational complexity without any notable loss in performance [9].

Distinct from these approaches which are all based on MRE, in [11], Li and Bar-Shalom propose a hybrid conditional averaging (HYCA) [12] based approach for the optimization of detection thresholds. A comprehensive comparison of MRE and HYCA-based static and dynamic threshold optimization schemes can be found in [13]. Yet another quite different approach is presented in [14] by Willett et al. where they feed the spatial (a posteriori) information of the tracking filter, back to a Bayesian detector as an a priori information. This results in a spatially adaptive detection threshold adjustment scheme. The effect is that the threshold is decreased near locations where the target is expected and increased near locations where it is unexpected.

In all aforementioned studies [5,7,15,11,13,14], it is implicitly assumed that the model describing the target motion dynamics is fairly well known to the filter. Hence, no explicit modeling uncertainty (or *modeling error*) is assumed. This can be a reasonable assumption if the target is following a single fixed motion pattern (such as linear motion or fixed radius turns). When the target is *maneuvering* with motion pattern transitions, however, this assumption clearly fails. The literature devoted to solving the *maneuver* problem is abundant with the works ranging from classical "two-moments" representation framework [1,3,16,17] to the recently popular so-called sequential Monte Carlo methods [18–22]. In the proposed solutions, the maneuver is treated mainly in three different ways. In the first treatment, it is modeled as a random process which enters the state dynamics as an additional *process noise*. In this case, the task turns out to be either readjusting the process noise level in a continuous space (called *continuous level adjustment*) or switching between several discrete noise levels (called *discrete level adjustment*) [17]. In the second treatment, the maneuver is modeled as a constant deterministic acceleration input continuing over a certain period of time [23]. Here, the unknown acceleration input is estimated either separately by another filter or simultaneously by the same filter through state augmentation. Then, the state estimation is corrected with this estimated input. Different than these two treatments, the third one uses a multiple model (MM) filtering approach [24]. Here, multiple filters, each matched to a different motion model, are run in parallel and their outputs are combined to obtain the global estimate. The algorithms in this category are proven to be superior to the previous two approaches. In particular, the interacting multiple model (IMM) structure [25]

provides an impressive performance with less computational complexity among its alternatives.

In the present paper, considering the aforementioned advantages, we pick the MM filtering approach as our focus and attempt to extend the formulation presented in [7] for the maneuvering target case. We hence propose a novel tracker-aware detector threshold optimization scheme for MM-based tracking of maneuvering targets in clutter. The proposed optimization scheme is applicable for any MM filtering structure which uses PDAFs as modules. We present the experimental results particularly for the IMM-PDAF. With this solution approach, the false alarm probability of the detector is optimized at each time step by feeding back information from the tracker. The detector hence operates in a *tracker-aware* manner. We consider an important transient performance criterion: *Track loss percentage* and show that such a feedback notably improves the robustness of IMM-PDAF against track loss especially in low SNR conditions.

The paper is organized as follows: The problem formulation is given in Section 2. In Section 3, we present the proposed tracker-aware optimization scheme for tracking maneuvering targets in clutter. The simulation results and their implications are discussed in Section 4, and finally, the concluding remarks are given in Section 5.

2. Problem formulation

We develop our formulation under the following assumptions:

- The state of the target of interest, of dimension n_x, is assumed to make its transition in time according to the equation

$$x(k)=F[M(k)]x(k-1)+G[M(k)]v(k-1,M(k)) \tag{1}$$

where $M(k)\in\{1,2,\ldots,r\}$ is a discrete-time switching random process which represents the system mode at k (i.e., the model in effect *during* the sampling period ending at time step k), and $\{v(k)\}$, called *process noise*, is a white sequence with $v(k)\sim\mathcal{N}(0,Q(k))$.[1] The linear system dynamics represented by state transition matrix F and process noise gain matrix G depends on the system mode.[2] The initial state $x(0)$, which is generally unknown, is modeled as $x(0)\sim\mathcal{N}(\hat{x}(0|0), P(0|0))$ where the mean $\hat{x}(0|0)$ and the covariance $P(0|0)$ are assumed to be known.
- The true (i.e., target originated) measurement, of dimension n_z, is given by

$$z(k)=Hx(k)+w(k) \tag{2}$$

where $\{w(k)\}$, called the *measurement noise*, is a white sequence with $w(k)\sim\mathcal{N}(0,R(k))$ and H, assumed constant, is the measurement matrix linking state and measurement vectors. Clearly, the measurement equation does not depend on the system mode.
- The two noise sequences $\{v(k)\}$ and $\{w(k)\}$ and the initial state $x(0)$ are assumed to be *mutually independent* for all k.
- At each time step k, the true measurement defined in (2) is available with a known *detection probability possibly* less than unity, i.e., $P_D(k)\le 1$.
- *False alarm* or *clutter* lead to false measurements. The locations of these measurements are modeled as random variables which are *independent identically distributed* (i.i.d.) with uniform spatial distribution over the *common validation gate*,[3] which is a hyper-ellipsoid in the measurement space, defined by [1, p. 95]

$$\mathcal{R}(k)\triangleq\{z(k) : [z(k)-\hat{z}_C(k|k-1)]^T S_C^{-1}(k)[z(k)-\hat{z}_C(k|k-1)]\le\gamma_G\} \tag{3}$$

where γ_G is the *gate threshold*. Here, $\hat{z}_C(k|k-1)$ is the center of the common gate (predicted measurement) and $S_C(k)$ is the associated covariance with $z(k)-\hat{z}_C(k|k-1)$ where $z(k)$ is the true measurement given in (2). Different techniques in obtaining a *common* validation region in multiple model filtering can be found, for example in [28].
- Assuming that $\lambda(k)$ and $V(k)$ are the spatial clutter density and the volume of the common validation gate at time step k, respectively, the number of false measurements at any time step k, denoted by m_k^F, is modeled as a random variable with probability mass function (pmf) $\mu_F(m_k^F;\lambda(k)V(k))$ where $\mu_F(m;\overline{m})$ denotes the Poisson pmf for the dummy variable m with mean $\overline{m}$, i.e.,

$$\mu_F(m;\overline{m})\triangleq\frac{e^{-\overline{m}}\overline{m}^m}{m!}. \tag{4}$$

- $M_j(k)\triangleq\{M(k)=j\}$ denotes the event that the model j is in effect at k.
- The *mode jump process* $M(k)$ is a Markov chain with known transition probabilities

$$\pi_{ij}\triangleq\Pr\{M_j(k)|M_i(k-1)\}. \tag{5}$$

Now, we define the tracker-aware detection threshold optimization problem as follows. We seek an optimum operating false alarm probability such that

$$P_{FA}^*(k)=\underset{P_{FA}}{\operatorname{argmin}}\left[\mathrm{E}[\|x(k)-\hat{x}(k|k)\|^2\,|Z^{k-1}]\right],\quad\text{subject to,}$$

$$P_D(k)=f_{ROC}(P_{FA}(k),\zeta(k))\quad\text{and}\quad 0\le P_{FA}(k)\le 1, \tag{6}$$

where $\hat{x}(k|k)$ is the state estimated by a multiple model filtering algorithm which uses the PDAFs as *modules* [1] (or *elemental filters* [27]), such as IMM-PDAF, and Z^{k-1} is the cumulative set of commonly validated measurements

[1] The common notation $x\sim\mathcal{N}(\overline{x},\Sigma)$ means that "the random variable x is normally (Gaussian) distributed with mean $\overline{x}$ and covariance Σ."

[2] Here, $x(k)$ and $M(k)$ are called the *base state* and the *modal state* [26], respectively. As $x(k)$ is continuous-valued and $M(k)$ is discrete-valued, the overall state $\phi(k)\triangleq[x(k)^T\ M(k)^T]^T$ is said to be *hybrid* [27].

[3] In a multiple model PDAF structure, each mode-matched filter normally suggests its own gate centered at its predicted measurement. But a *common* validation gate for all mode-matched filters is necessary as the calculated mode likelihood functions should be the pdf of the *same* set of measurements (for further explanation, see e.g., [1, p. 200]).

(i.e., the measurements falling inside the validation region defined in (3)) upto and including time $k-1$. Our aim is to find an optimum false alarm probability, which in turn determines the detection threshold for a given SNR (ζ) value. The equality constraint of the optimization problem is the receiver operating characteristic (ROC) relation of a radar detector and the inequality one is used to guarantee that the resulting false alarm is a valid probability.

Remark 1. The optimization problem defined in (6) is a multiple model filtering extension of the *prior detection threshold optimization* problem defined in [7] where the same problem is formulated for single model (PDAF) case.

Remark 2. Note that, the optimum false alarm probability, $P_{FA}^*(k)$ hence the optimum threshold for the detector at time k is used to produce measurements at time k. Therefore, taking the expectation in (6) conditioned on Z^{k-1} but not on Z^k makes the optimization more feasible from the practical implementations (i.e., causality) point of view, as the latter case requires a more time-demanding iterative procedure for finding the optimum threshold value.

3. Tracker-aware detector threshold optimization

The minimization part of the optimization problem defined in (6) can be rewritten as

$$P_{FA}^*(k)=\underset{P_{FA}}{\operatorname{argmin}}\left[\mathrm{E}[\|x(k)-\hat{x}(k|k)\|^2|Z^{k-1}]\right] \tag{7}$$

$$P_{FA}^*(k)=\underset{P_{FA}}{\operatorname{argmin}}\left[\mathrm{E}[\mathrm{tr}\{P(k|k)\}|Z^{k-1}]\right] \tag{8}$$

$$P_{FA}^*(k)=\underset{P_{FA}}{\operatorname{argmin}}\left[\mathrm{tr}\left\{\mathrm{E}[P(k|k)|Z^{k-1}]\right\}\right] \tag{9}$$

where $\mathrm{tr}\{\cdot\}$ is the trace operator and $P(k|k)$ is the covariance associated with $\hat{x}(k|k)$. Assuming that the model in effect can only be one of the r possible models, the events $M_j(k)$, $j=1,2,\ldots,r$ are *mutually exclusive*, i.e., $\Pr\{M_i(k), M_j(k)\}=0$, $\forall i\neq j$ and *exhaustive*, i.e., $\sum_{j=1}^{r}\Pr\{M_j(k)\}=1$. So, we can apply total expectation theorem to (9) as

$$P_{FA}^*(k)=\underset{P_{FA}}{\operatorname{argmin}}\left[\mathrm{tr}\left\{\sum_{j=1}^{r}\mathrm{E}[P(k|k)|M_j(k),Z^{k-1}]\Pr\{M_j(k)|Z^{k-1}\}\right\}\right]$$

$$P_{FA}^*(k)=\underset{P_{FA}}{\operatorname{argmin}}\left[\mathrm{tr}\left\{\sum_{j=1}^{r}\mathrm{E}[P^j(k|k)|Z^{k-1}]\mu_j(k|k-1)\right\}\right]$$

$$P_{FA}^*(k)=\underset{P_{FA}}{\operatorname{argmin}}\left[\mathrm{tr}\left\{\sum_{j=1}^{r}\overline{P}^j(k|k)\mu_j(k|k-1)\right\}\right]$$

$$P_{FA}^*(k)=\underset{P_{FA}}{\operatorname{argmin}}\left[\sum_{j=1}^{r}\mathrm{tr}\{\overline{P}^j(k|k)\}\mu_j(k|k-1)\right] \tag{10}$$

where $\mu_j(k|k-1)\triangleq\Pr\{M_j(k)|Z^{k-1}\}$, $j=1,2,\ldots,r$ are the *predicted* model probabilities. The term $\overline{P}^j(k|k)$, which is a deterministic version of the model-conditioned covariance $P^j(k|k)$, can be further substituted by either MRE [5] or HYCA [12] approximations. For the MRE case, this term can be approximately written as [5]

$$\begin{aligned}\overline{P}^j(k|k)&=\overline{P}^j_{MRE}(k|k)\triangleq\mathrm{E}[P^j(k|k)|Z^{k-1}]\\&\approx P^j(k|k-1)-q_2(P_{FA}(k)N_C^j(k),P_D(k))W^j(k)S^j(k)W^j(k)^T\end{aligned} \tag{11}$$

where $q_2(\cdot,\cdot)$ is a scalar, called the *information reduction factor* (IRF) [1], which takes the values between 0 and 1, and defined in an earlier study [5] as

$$\begin{aligned}q_2(P_{FA}(k)N_C(k),P_D(k))\triangleq\frac{P_D(k)c_{n_z}}{(2\pi)^{n_z/2}}\sum_{m_k=1}^{\infty}\mu_F(m_k-1;P_{FA}(k)N_C(k))\\\times\left(\frac{n_z}{g^{n_z}}\right)^{m_k-1}I_2(P_{FA}(k)N_C(k),P_D(k),m_k)\end{aligned} \tag{12}$$

with

$$\begin{aligned}I_2(P_{FA}N_C(k),P_D,m_k)\triangleq\int_0^g\cdots\int_0^g\frac{\exp(-r_1^2)r_1^2}{b(P_{FA}N_C(k),P_D)+\sum_{j=1}^{m_k}\exp(-r_j^2/2)}\\\times(r_1r_2\ldots r_{m_k})^{n_z-1}dr_1dr_2\ldots dr_{m_k}\end{aligned} \tag{13}$$

$$b(P_{FA}N_C(k),P_D)\triangleq(2\pi)^{n_z/2}\frac{P_{FA}N_C(k)}{c_{n_z}g^{n_z}}\frac{(1-P_DP_G)}{P_D} \tag{14}$$

where $c_{n_z}\triangleq\pi^{n_z/2}/\Gamma(n_z/2+1)$, with $\Gamma(\cdot)$ being the gamma function, is the volume of the n_z-dimensional unit hypersphere ($c_1=2, c_2=\pi, c_3=4\pi/3$, etc.). The terms $W^j(k)$ and $S^j(k)$ are, respectively, the Kalman gain and innovation covariance corresponding to the jth model-matched PDAF at time step k. Furthermore,

$$N_C^j(k)\triangleq\frac{V^j(k)}{V_C}=\frac{c_{n_z}g^{n_z}|S^j(k)|^{1/2}}{V_C} \tag{15}$$

is the number of resolution cells enclosed by the validation gate defined by the jth model. The volume of this validation gate at time step k is $V^j(k)$ and V_C is the resolution cell volume which is assumed to be constant. Substituting (11) into (10), we have

$$\begin{aligned}P_{FA}^*(k)=\underset{P_{FA}}{\operatorname{argmin}}\left[\sum_{j=1}^{r}\mathrm{tr}\{P^j(k|k)\}\mu_j(k|k-1)-\sum_{j=1}^{r}q_2(P_{FA}(k)N_C^j(k),P_D(k))\right.\\\left.\times\mathrm{tr}\{W^j(k)S^j(k)W^j(k)^T\}\mu_j(k|k-1)\right].\end{aligned} \tag{16}$$

Note that the first summation does not depend on P_{FA} and, therefore, it can be removed from the optimization. Furthermore, since $W^j(k)S^j(k)W^j(k)^T\geq 0$ $\forall j$ the terms in the second summation are all non-negative. So the final form of the problem can be expressed as

$$\begin{aligned}P_{FA}^*(k)=\underset{P_{FA}}{\operatorname{argmax}}\left[\sum_{j=1}^{r}q_2(P_{FA}(k)N_C^j(k),P_D(k))\right.\\\left.\times\mathrm{tr}\{W^j(k)S^j(k)W^j(k)^T\}\mu_j(k|k-1)\right],\quad\text{subject to,}\end{aligned}$$

$$P_D(k)=f_{ROC}(P_{FA}(k),\zeta(k))\quad\text{and}\quad 0\leq P_{FA}(k)\leq 1. \tag{17}$$

Note that the optimization problem defined in (17) is one dimensional. The functional form of the IRF given in (12),

is mathematically intractable to differentiate with respect to P_{FA}. However, it can be evaluated numerically at any point of interest provided that the infinite summation is truncated at a "sufficiently" high value. Therefore, any line search algorithm that requires only the values of the objective function, such as, Golden-Section or Fibonacci Search methods [8], can be applied to this problem. Provided that the cost function is *unimodal*,[4] these algorithms converge to the global optimum.

Eq. (17) and the associated derivation are our main contributions in the present study and constitute the feedback path in Fig. 1 for MM tracking filters which use the PDAF modules. By solving this one dimensional numerical optimization problem at every time step k, it is possible to generate the optimal P_{FA} settings for the detector such that the tracker, which is a r-model MM filter, performs optimally for a maneuvering target with r possible modes. Note that the predicted model probabilities $\{\mu_j(k|k-1)\}_{j=1}^{r}$ can either be easily calculated from or directly produced within any MM filtering structure ranging from *static multiple model estimators* [17, p. 441] to the *dynamic* ones such as nth order generalized pseudo-Bayesian (GPBn) methods [29,30] and the well-known interacting multiple model (IMM) filter [25]. So, our derivation, hence our contribution is general in the sense that it is independent of the type of MM filtering structure used in the tracking side.

The simulation-based experimental results in the next section presents the practical consequence of this proposed feedback system as compared with the conventional feed-forward structure.

4. Simulation results

We consider an air traffic control (ATC) scenario, illustrated in Fig. 2. Here, an aircraft with an initial position of $p_T(0)=[0 \quad 25\,000]^T$ m, flies eastward with a speed of $\|v_T\|=150$ m/s for a duration of 150 s. Then, it performs a coordinated turn with a turn rate of $\Omega=1$ deg/s (which amounts to $\sim 0.26g$ maneuver at this speed) for 150 s. Finally, it flies straight towards southwest for another 150 s.

In generating this motion, we use a white noise acceleration (WNA) model for the straight parts of the motion and a constant turn rate coordinated turn (CT) model[5] for the maneuvering part. In both WNA and CT models, we assume a process noise with a standard deviation of $q=0.01$ m/s^2 in linear portions of the state transition.

The radar is located at $l_R=[23\,400 \quad 16\,400]^T$ m, which corresponds approximately to the center of the coordinated turn maneuver. We assume that the radar provides position only measurements for every $T=3$ s with a *rectangular*[6] resolution cell of 50 m in each coordinate

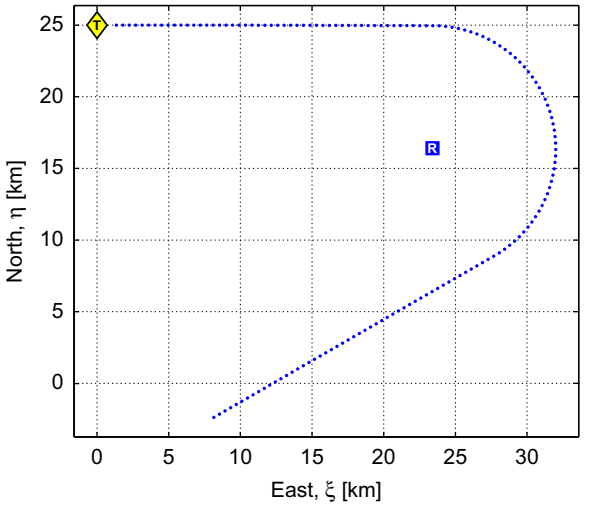

Fig. 2. A sample air traffic control (ATC) scenario: The diamond marker "T" and the square marker "R" denote initial aircraft (or target) position and radar location, respectively. The motion trajectory consists of three sections corresponding to two different dynamic models (modes) for the aircraft.

which implies that the resolution cell volume is constant and equal to $V_C=2500$ m^2.

We assume that SNR depends only on range as $\zeta(r)=C_\zeta/r^4$ where C_ζ is the SNR constant representing all the other factors in the SNR equation and r is the range to the target. The variations of the radar to aircraft range and that of the target SNR for $C_\zeta=4\times10^{17}$ are shown in Fig. 3. The minimum and maximum target ranges are reported to be as $r_{min}\approx 8.5$ km and $r_{max}\approx 24$ km, respectively. Note that, at the beginning and at the end of the motion, SNR is very low as the target range is high. On the other hand, as the target approaches the radar, the SNR increases, and it reaches and stays at the maximum value during the coordinated turn maneuver. The minimum and maximum SNR values for different values of C_ζ are listed in Table 1. These are the different SNR conditions considered in the experiment. We chose deliberately very low ζ_{min} values to be able to illustrate the effect of threshold optimization on the system performance for very difficult SNR scenarios.

As a detector, a Neyman–Person type detector is considered and its ROC relation is given by[7]

$$P_D=P_{FA}^{1/(1+\zeta)}. \tag{18}$$

The quantization errors induced by the finite resolution of the sensor is modeled by the measurement noise, $w(k)$. Assuming that the true measurement is uniformly distributed in the resolution cell [1, p. 472], the error

[4] Experimentally, it can be observed that the cost function in (17) satisfies this requirement.

[5] While simulating the motion, we do not add any process noise component to the turn rate. In the case of adding a noise to the turn rate, the motion model is often referred to as *nearly coordinated turn* (NCT) model [17, p. 467].

[6] We assume rectangular resolution cells to have a linear measurement model.

[7] This ROC curve relation is valid under the assumption of *homogeneous* and *Gaussian* background detector noise, a Swerling-I target fluctuation and *square-law* detection scheme. In radar detection theory, these assumptions are made frequently when obtaining the ROC curves for a specific detector [4].

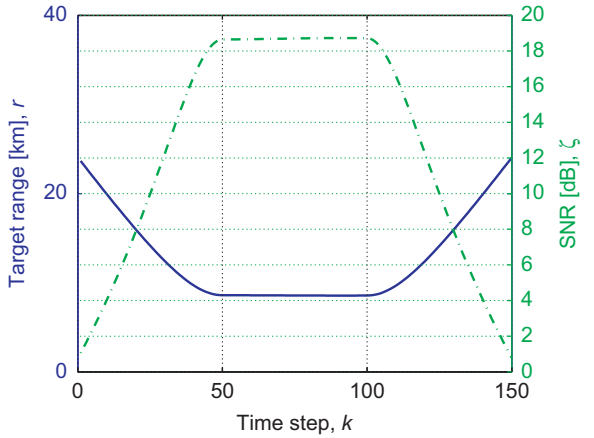

Fig. 3. The variation of the range between target and radar, and that of SNR for $C_\zeta = 4 \times 10^{17}$ case.

Table 1
Minimum and maximum SNR values for different values of the SNR constant, C_ζ.

C_ζ (m^4)	ζ_{min} (dB)	ζ_{max} (dB)
4×10^{17}	0.78	18.73
5×10^{17}	1.75	19.70
6×10^{17}	2.54	20.49
7×10^{17}	3.21	21.16
8×10^{17}	3.79	21.73
9×10^{17}	4.30	22.25
1×10^{18}	4.76	22.71

covariance of $w(k)$ is taken as

$$R = \begin{bmatrix} (\Delta r_\xi/\sqrt{12})^2 & 0 \\ 0 & (\Delta r_\eta/\sqrt{12})^2 \end{bmatrix} \tag{19}$$

for all k, where Δr_ξ and Δr_η are the range resolutions, assumed 50 m, in East and North directions, respectively.

In the filtering side, we design two elemental PDAF filters, named as PDAF-Q001 and PDAF-Q3, which use a second order linear kinematic model (WNA) with process noise standard deviations of $q = 0.01$ and 3 m/s^2, respectively. Each filter is initialized by means of the *two point differencing* [17, p. 247] method. These elemental filters are used as *modules* inside the MM filtering structure and are designed to track the target in its quiescent and maneuvering modes, respectively.[8] Note that the maneuvering model filter, PDAF-Q3 is designed to match (conservatively) for the maximum maneuver expected, i.e., ~ 2.6 m/s^2 in the scenario. As a multiple model filtering structure, we use an IMM filter whose Markov chain

[8] To track the maneuvering mode, a better approach is to use a coordinated turn (CT) model. This model is nonlinear and hence requires an extended Kalman filter (EKF) based PDAF with the associated impacts of online linearization.

Table 2
Compared tracking systems.

System name	P_{FA}^d
IMM-PDAF-E8	$P_{FA}(k) = 10^{-8}$
IMM-PDAF-E6	$P_{FA}(k) = 10^{-6}$
IMM-PDAF-E4	$P_{FA}(k) = 10^{-4}$
IMM-PDAF-E2	$P_{FA}(k) = 10^{-2}$
IMM-PDAF-OP	$P_{FA}(k)$ is set as given in (17)

transition matrix is given by

$$\Pi = \begin{bmatrix} 1-1/\mathrm{E}[\tau_Q] & 1/\mathrm{E}[\tau_Q] \\ 1/\mathrm{E}[\tau_M] & 1-1/\mathrm{E}[\tau_M] \end{bmatrix} \tag{20}$$

where $\mathrm{E}[\tau_Q]$ and $\mathrm{E}[\tau_M]$ are the expected *sojourn times* [17, p. 487] (in unit of sampling interval) of the underlying Markov chain in quiescent and maneuvering modes, respectively. For our case, we take these values as $\mathrm{E}[\tau_Q] = 100$ and $\mathrm{E}[\tau_M] = 50$. Furthermore, the initial model probabilities are taken as $\mu(0) = [0.5 \quad 0.5]^T$.

In the experiment, we compare the proposed threshold optimization scheme with conventional approaches, where IMM-PDAFs are used with *conventional detectors*.[9] The compared tracking systems are listed in Table 2.

The first four tracking systems are conventional and use heuristically selected desired false alarm probabilities ranging from 10^{-8} to 10^{-2} while the last system uses a tracker-aware detector whose false alarm probability is fed back at every time step from the tracking filter. The 100 Monte Carlo runs are performed over the scenario presented in Fig. 2 for each of the SNR conditions listed in Table 1. Track loss condition is asserted for the ith Monte Carlo run if the average estimation error for that simulation run exceeds the average measurement error for the the same run. Then, the track loss percentage (TLP) is defined as the ratio of the number of Monte Carlo runs for which track loss occurs to the total number of Monte Carlo runs performed. The average RMS position error values are calculated from *track loss free* runs.

Track loss percentages and average RMS position errors for different values of C_ζ are given in Tables 3 and 4, respectively.

Here, KF-BASELINE denotes the *true mode-matched* Kalman filter with perfect data association and represents the ultimate performance upper limit which can never be achieved in practice. For a better illustration of the performances of the algorithms, for $C_\zeta = 1 \times 10^{18}$ case, TLP and average RMS position error value pairs are plotted as performance points in Fig. 4. Clearly, the KF-BASELINE point in this plane represents the performance target for all algorithms and a better algorithm is one that is closer to the KF-BASELINE point. It can be noted from Fig. 4 that the proposed system IMM-PDAF-OP shows a considerably improved performance in terms of the TLP measure while preserving a favorably comparable performance in terms of the average RMS position error

[9] By the conventional detector, we mean the detector whose desired false alarm probability, P_{FA}^d is set heuristically to a constant value.

Table 3
Track loss percentages (%).

System name	SNR constant, C_ζ (m^4)						
	1×10^{18}	9×10^{17}	8×10^{17}	7×10^{17}	6×10^{17}	5×10^{17}	4×10^{17}
KF-BASELINE	0	0	0	0	0	0	0
IMM-PDAF-E8	96	94	98	100	100	99	100
IMM-PDAF-E6	80	80	85	95	97	100	100
IMM-PDAF-E4	42	57	61	80	81	92	96
IMM-PDAF-E2	67	73	81	92	93	99	99
IMM-PDAF-OP	40	41	51	73	75	90	97

Table 4
Average RMS position errors (m).

System name	SNR constant, C_ζ (m^4)						
	1×10^{18}	9×10^{17}	8×10^{17}	7×10^{17}	6×10^{17}	5×10^{17}	4×10^{17}
KF-BASELINE	12.3515	12.1405	12.1534	12.0800	12.0239	12.1279	12.1829
IMM-PDAF-E8	17.5725	19.0719	17.8586	N/A	N/A	17.4377	N/A
IMM-PDAF-E6	18.9671	18.8323	19.0789	19.7609	18.2498	N/A	N/A
IMM-PDAF-E4	19.2023	18.8086	19.4615	19.5313	19.5268	18.6406	19.6058
IMM-PDAF-E2	18.8176	19.5101	18.3066	19.3564	17.4124	18.9084	15.8702
IMM-PDAF-OP	18.2771	18.4509	18.8909	19.1967	18.7658	18.6134	16.4778

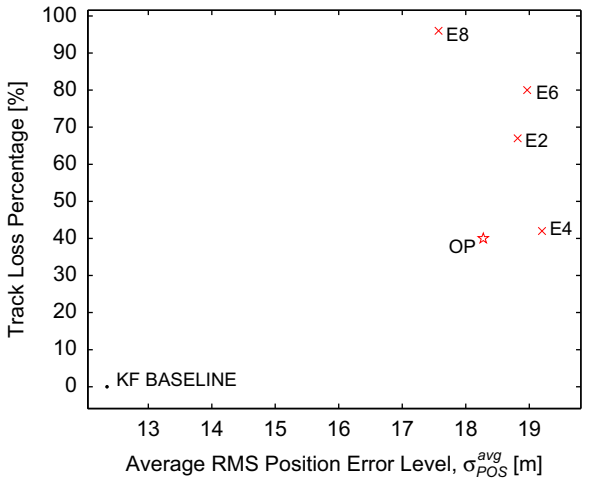

Fig. 4. The performances of the algorithms in terms of track loss percentage and average RMS position error for the $C_\zeta = 1\times10^{18}$ case.

measure. This can be interpreted as a more robust operation of the filter against track loss. In Table 5, the average RMS position errors are given for each motion legs separately for $C_\zeta = 1\times10^{18}$ case. Here, Leg-1 and Leg-3 corresponds to the non-maneuvering (NM) parts of the motion, while Leg-2 corresponds to the maneuvering (M) part. Considering also its lower TLP value, it can be noted that the proposed tracking system operates fairly good in both maneuvering and non-maneuvering parts of the motion.

The optimum false alarm probabilities suggested by the proposed optimization scheme are given in Fig. 5 for different values of C_ζ. We have observed in our simulations that during the maneuvering part of the motion, which corresponds to the time steps between 51 and 100, the volume of the validation gate increases. We interpret that the volume increases due to the mismatch between the filter-assumed models and the true mode of the system. In the classical approach, there is no aspect of the algorithm countering this trend, and it is likely that this increase continues until the point where the filter becomes unstable. The proposed optimization on the other hand, suggests to lower the desired P_{FA} value in this critical region, which in turn reduces the number of false measurements falling inside the validation gate. It is our belief that this effect acts as form of negative feedback, which bounds the volume of the validation gate, which in turn stabilizes the filter. This observation is also consistent with the significant performance gain we observe in Fig. 4 in terms of the track loss percentage. Another mechanism observed in Fig. 5 is that the optimal P_{FA} values suggested by the proposed optimization scheme are conversely proportional to the operating SNR. When the SNR decreases the detection probability of target also decreases. So, the optimization scheme in this case suggests to lower the detection thresholds (by equivalently increasing the desired false alarm probability values for the detector) so that to increase the chance of target detection in severe (low) SNR conditions.

Considering the computational load of the proposed scheme, we observed that the proposed algorithm needs approximately 14 times much computational power as compared to conventional approaches. More specifically, one cycle (i.e., one time step) of IMM-PDAF-OP takes about 23 ms while one cycle of any one of classical IMM-PDAF-EX takes about 1.6 ms, on the average in our MATLAB implementations which run in a computer with Intel Centrino Duo 1.67 GHz processor and 2 GB RAM.

Table 5
Average RMS position errors (m) in different motion legs for $C_\zeta = 1 \times 10^{18}$ case.

System name	TLP (%)	Leg-1 (NM) (k=1:50)	Leg-2 (M) (k=51:100)	Leg-3 (NM) (k=101:150)	Overall (k=1:150)
KF-BASELINE	0	9.1970	18.7725	9.0851	12.3515
IMM-PDAF-E8	96	17.8735	20.7333	14.1106	17.5725
IMM-PDAF-E6	80	21.1411	21.3524	14.4079	18.9671
IMM-PDAF-E4	42	22.1158	21.4354	14.0556	19.2023
IMM-PDAF-E2	67	17.6239	24.4383	14.3907	18.8176
IMM-PDAF-OP	40	20.3334	21.1864	13.3117	18.2771

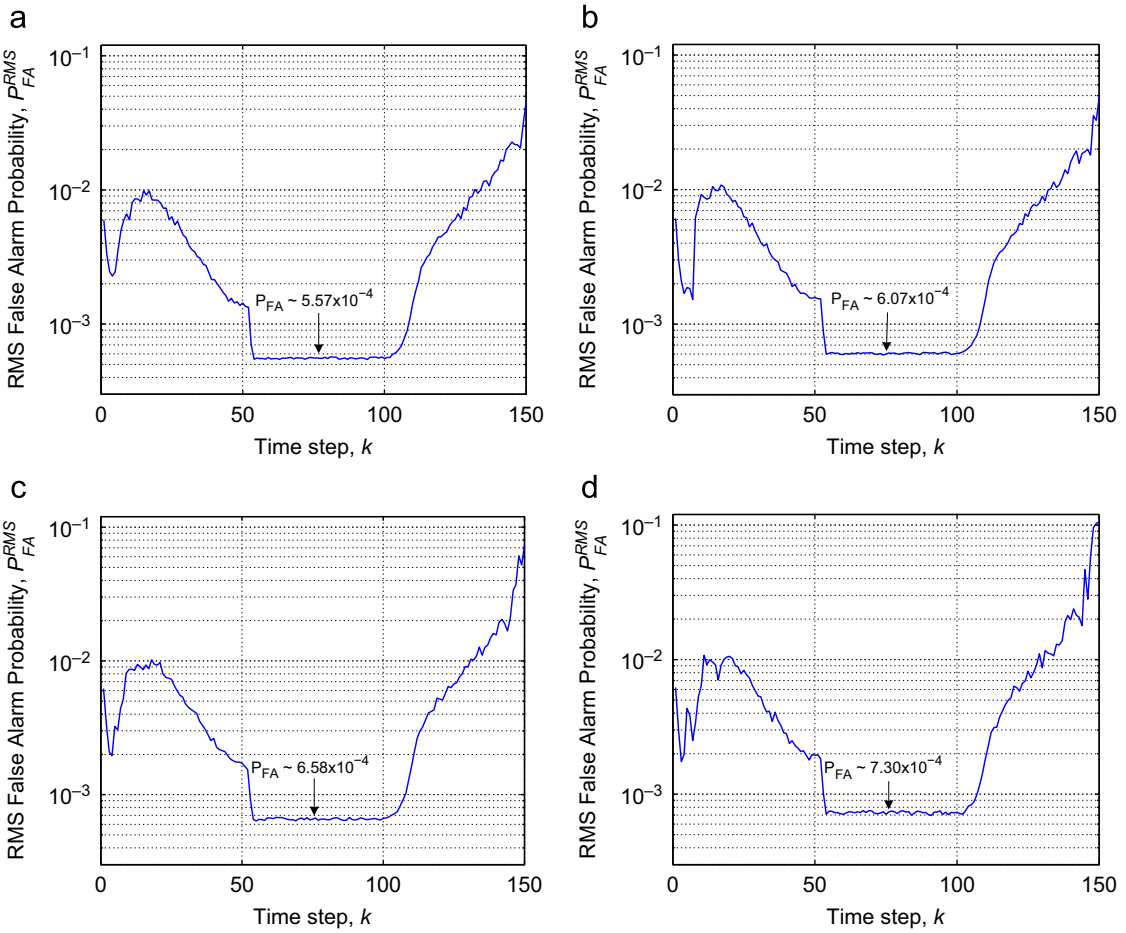

Fig. 5. The optimum false alarm probabilities suggested by the proposed threshold optimization scheme for (a) $C_\zeta = 1 \times 10^{18}$ m^4, (b) $C_\zeta = 9 \times 10^{17}$ m^4, (c) $C_\zeta = 8 \times 10^{17}$ m^4 and (d) $C_\zeta = 7 \times 10^{17}$ m^4 cases. The average P_{FA} values during maneuvering part of the motion are also shown for each case.

5. Conclusion

In this paper, the ideas applied previously for the optimization of detection thresholds for non-maneuvering target tracking in clutter are extended to maneuvering target tracking case. The proposed extension is fully integrated into MM filtering structures which use the PDAFs as modules. The solution utilizes the *soft* model switching mechanism inherently available in MM filtering. In the experimental study this tracker-aware optimization scheme is applied particularly to the IMM-PDAF case by means of a realistic simulation setup. The promising results suggest that the presented extension performs notably better than the conventional approach to MM maneuvering target tracking in clutter, in particular for the transient performance of the IMM-PDAF filter characterized by the track loss percentage of the filter, at a cost of increased computational power.

References

[1] Y. Bar-Shalom, X.R. Li, Multitarget-Multisensor Tracking: Principles and Techniques, YBS Publishing, Box U-157, Storrs, CT 06269-3157, 1995.

[2] M.A. Richards, Fundamentals of Radar Signal Processing, McGraw-Hill, 2005.
[3] S.S. Blackman, R. Popoli, Design and Analysis of Modern Tracking Systems, Artech House, Norwood, MA, 1999.
[4] P.K. Varshney, Distributed Detection and Data Fusion, Springer Verlag, New York, Inc., 1997.
[5] T.E. Fortmann, Y. Bar-Shalom, M. Scheffe, S. Gelfand, Detection thresholds for tracking in clutter—a connection between estimation and signal processing, IEEE Transactions on Automatic Control AC 30 (3) (1985) 221–229.
[6] Y. Bar-Shalom, E. Tse, Tracking in a cluttered environment with probabilistic data association, Automatica 11 (1975) 451–460.
[7] S.B. Gelfand, T.E. Fortmann, Y. Bar-Shalom, Adaptive detection threshold optimization for tracking in clutter, IEEE Transactions on Aerospace and Electronic Systems 32 (1996) 514–523.
[8] M. Bazaraa, H. Sherali, C. Shetty, Nonlinear Programming Theory and Algorithms, Wiley, 2006.
[9] M. Şamil Aslan, A. Saranlı, B. Baykal, Tracker-aware adaptive detection: an efficient closed-form solution for the Neyman–Pearson case, Digital Signal Processing 20 (5) (2010) 1468–1481.
[10] D.J. Kershaw, R.J. Evans, A contribution to performance prediction for probabilistic data association tracking filters, IEEE Transactions on Aerospace and Electronic Systems 32 (3) (1996) 1143–1148.
[11] X.R. Li, Y. Bar-Shalom, Detection threshold selection for tracking performance optimization, IEEE Transactions on Aerospace and Electronic Systems 30 (1994) 742–749.
[12] X.R. Li, Y. Bar-Shalom, Stability evaluation and track life of the PDAF for tracking in clutter, IEEE Transactions on Automatic Control 36 (1991) 588–602.
[13] M. Şamil Aslan, A. Saranlı, Characterization of NSPP-based detector threshold optimization for tracking a non-maneuvering target in clutter, IEEE Transactions on Aerospace and Electronic Systems, in press, doi:0018-9251/11.
[14] P. Willett, R. Niu, Y. Bar-Shalom, Integration of Bayes detection with target tracking, IEEE Transactions on Signal Processing 49 (1) (2001) 17–29.
[15] M. Şamil Aslan, A. Saranlı, B. Baykal, Optimal tracker-aware radar detector threshold adaptation: a closed-form solution, in: International Conference on Information Fusion, 2008, pp. 470–477.
[16] Y. Bar-Shalom, W.D. Blair (Eds.), Multitarget-Multisensor Tracking: Applications and Advances Volume III, Artech House Inc., 2000.
[17] Y. Bar-Shalom, X.R. Li, T. Kirubarajan, Estimation with Applications to Tracking and Navigation, John Wiley & Sons, Inc., 2001.
[18] A. Doucet, N.J. Gordon, V. Krishnamurthy, Particle filters for state estimation of jump markov linear systems, IEEE Transactions on Signal Processing 49 (3) (2001) 613–624.
[19] M.R. Morelande, S. Challa, Manoeuvring target tracking in clutter using particle filters, IEEE Transactions on Aerospace and Electronic Systems 41 (1) (2005) 252–270.
[20] Y. Yu, Q. Cheng, Particle filters for maneuvering target tracking problem, Signal Processing 86 (2006) 195–203.
[21] S. Mcginnity, G.W. Irwin, Multiple model bootstrap filter for maneuvering target tracking, IEEE Transactions on Aerospace and Electronic Systems 36 (3) (2000) 1006–1012.
[22] D. Angelova, T. Semerdjiev, V. Jilkov, E. Semerdjiev, Application of a Monte Carlo method for tracking maneuvering target in clutter, Mathematics and Computers in Simulation 55 (2001) 15–23.
[23] Y.T. Chan, A.G.C. Hu, J.B. Plant, A Kalman filter based tracking scheme with input estimation, IEEE Transactions on Aerospace and Electronic Systems AES 15 (2) (1979) 237–244.
[24] X.R. Li, V.P. Jilkov, Survey of maneuvering target tracking. Part V: multiple-model methods, IEEE Transactions on Aerospace and Electronics Systems 41 (4) (2005) 1255–1321.
[25] H.A.P. Blom, Y. Bar-Shalom, The interacting multiple model algorithm for systems with Markovian switching coefficients, IEEE Transactions on Automatic Control 33 (8) (1988) 780–783.
[26] X.R. Li, Y. Bar-Shalom, Performance prediction of the interacting multiple model algorithm, IEEE Transactions on Aerospace and Electronic Systems 29 (3) (1993) 755–771.
[27] X.R. Li, Multitarget-Multisensor Tracking: Applications and Advances Volume III, Artech House, Inc., 2000, pp. 499–567 (Chapter 10).
[28] X. Wang, S. Challa, R. Evans, Gating techniques for maneuvering target tracking in clutter, IEEE Transactions on Aerospace and Electronic Systems 38 (3) (2002) 1087–1097.
[29] G.A. Ackerson, K.S. Fu, On state estimation in switching environments, IEEE Transactions on Automatic Control 15 (1) (1970) 10–17.
[30] J.K. Tugnait, Adaptive estimation and identification for discrete systems with Markov jump parameters, IEEE Transactions on Automatic Control 27 (5) (1982) 1054–1065.